Calculation of the optical response of atomic clusters using time-dependent density functional theory and local orbitals

Argyrios Tsolakidis, Daniel Sánchez-Portal,* and Richard M. Martin
Department of Physics and Materials Research Laboratory, University of Illinois at Urbana-Champaign, Urbana, Illinois 61801
(Received 24 September 2001; revised manuscript received 2 August 2002; published 26 December 2002)

We report on a general method for the calculation of the frequency-dependent optical response of clusters based upon time-dependent density functional theory (TDDFT). The implementation is done using explicit propagation in the time domain and a self-consistent program that uses a linear combination of atomic orbitals (LCAO). Our actual calculations employ the SIESTA program, which is designed to be fast and accurate for large clusters. We use the adiabatic local density approximation to account for exchange and correlation effects. Results are presented for the imaginary part of the linear polarizability, $\mathrm{Im}\,\alpha(\omega)$, and the dipole strength function, $S(\omega)$, of C_{60} and Na_8, and compared to previous calculations and to experiment. We also develop a method for the calculation of the integrated frequency-dependent second-order nonlinear polarizability for the case of a step function electric field, $\tilde{\gamma}_{\mathrm{step}}(\omega)$, and present results for C_{60}.

DOI: 10.1103/PhysRevB.66.235416 PACS number(s): 78.70.−g, 78.67.−n

I. INTRODUCTION

Although density functional theory[1,2] (DFT) is a very successful theory for the ground state properties, the excited states calculated within the Kohn-Sham scheme often are much less successful in describing the optical response and the excitation spectra. The solution to this problem, in principle, is the extension of DFT to the time-dependent systems. It is interesting to note that the first calculation[3] using time-dependent DFT (TDDFT) preceded any formal development and it relied heavily on the analogy with the time-dependent Hartree-Fock method. The first steps towards the formulation of TDDFT were done by Deb and Ghosh,[4,5] who focused on potentials periodic in time, and by Bartolotti,[6,7] who focused on adiabatic processes. Runge and Gross[8] established the foundations of TDDFT for a generic form of the time-dependent potential. TDDFT was further developed[9,10] to acquire a structure that is very similar to that of the conventional DFT. A very interesting feature of TDDFT, that does not appear in DFT, is the dependence of the density functionals on the initial state. For more information about TDDFT the reader is advised to read the authoritative reviews of Gross, Ullrich, and Gossmann[11] and Gross, Dobson, and Petersilka.[12]

The polarizability describes the distortion of the charge cloud caused by the application of an external field. It is one of the most important response functions because it is directly related to electron-electron interactions and correlations. In addition, it determines the response to charged particles and optical properties. A quantity of particular interest is the dipole strength function, $S(\omega)$, which is directly related to the frequency-dependent linear polarizability, $\alpha(\omega)$, by

$$\alpha(\omega)=\frac{e^2\hbar}{m}\int_0^\infty \frac{S(\omega')d\omega'}{\omega'^2-\omega^2}. \tag{1}$$

By taking the imaginary part of Eq. (1) we obtain

$$S(\omega)=\frac{2m}{\pi e^2\hbar}\omega\,\mathrm{Im}\,\alpha(\omega). \tag{2}$$

The dipole strength function, $S(\omega)$, is proportional to the photoabsorption cross section, $\sigma(\omega)$, measured by most experiments and, therefore, allows direct comparison with experiment. In addition, the integration of S over energy gives the number of electrons, N_e (*f-sum rule*), i.e.,

$$\int_0^\infty dE\,S(E)=\sum_i f_i=N_e, \tag{3}$$

where f_i are the oscillator strengths. This sum rule is very important because it provides an internal consistency test for the calculations, indicating the completeness and adequacy of the basis set used for the computation of the optical response.

Optical probes are some of the most successful experimental tools that allow access to the properties of clusters. Consequently, there are many calculations of the optical response of small atomic aggregates.[13] In particular, there exist several theoretical studies of the examples chosen here, C_{60} and Na_8. This allows us to calibrate the accuracy of our method in comparison with other computational schemes. Two of the first *ab initio* calculations within TDDFT were performed by Rubio *et al.*[14] and by Yabana and Bertsch.[15] Rubio *et al.*[14] calculated the *ab initio* photoabsorption cross sections of small silicon and alkali-metal clusters (Li, Na) using the time-dependent local density approximation (TDLDA). Yabana and Bertsch[15] performed calculations of the dipole response of atomic clusters and studied large sodium and lithium clusters and the C_{60} molecule using TDLDA and a real-time and -space approach. Shortly after, van Gisbergen *et al.*[16] calculated the dynamic hyperpolarizability of C_{60} using TDDFT. For small Na clusters, Vasiliev *et al.*[17] calculated the photoabsorption cross section using the time-dependent density functional response theory (TDDFRT) developed by Casida.[18] Of particular interest are the recent calculations of Moseler *et al.*,[19] who calculated the

 ©2002 The American Physical Society

photoabsorption cross sections of small sodium cluster cations at various temperatures using TDLDA in conjuction with *ab initio* molecular dynamics. The calculated spectra are obtained without using *ad hoc* line broadening or renormalization.

The purpose of this work is to propose a method that will have significant advantages for the calculation of the polarizability of large clusters, reducing considerably the computation time while retaining a reasonable accuracy. This paper is organized as follows: In Sec. II, we describe the method of calculation. In Sec. III, we present an overview of relevant calculations and the results of our calculation for C_{60} and Na_8. We compare our results with other calculations and experiments. In Sec. IV, we describe the calculation and present the results for the imaginary part of the integrated frequency-dependent second-order nonlinear polarizability for the case of a step function electric field, $\mathrm{Im}\,\tilde{\gamma}_{\mathrm{step}}(\omega)$, for C_{60}. In Sec. V, we give the conclusions.

II. METHOD OF CALCULATION

A. Electronic structure calculations

Our method involves the description of the electronic states using linear combination of atomic orbitals (LCAO). Because the size of the LCAO basis is small, the TDDFT calculations can be done efficiently using the techniques described below. The use of the LCAO basis leads to matrices with size considerably smaller than when other basis sets are used or when real-space grid methods are employed. Our scheme is based on the SIESTA code,[20–22] which is used to compute the initial wave functions and the Hamiltonian matrix for each time step. SIESTA is a general-purpose DFT code that uses a local basis, and has been specially optimized to deal with large systems. As such, it represents an ideal tool for treating large clusters. Core electrons are replaced by norm-conserving pseudopotentials[23] in the fully nonlocal Kleinman-Bylander[24] form, and the basis set is a general and flexible linear combination of numerical atomic orbitals (NAOs), constructed from the eigenstates of the atomic pseudopotentials.[21,25] The NAOs are confined, being strictly zero beyond a certain radius. In addition, the electron wave functions and density are projected onto a real-space grid in order to calculate the Hartree and exchange-correlation potentials and their matrix elements.

The use of confined NAOs is very important for the efficiency of the SIESTA code. With them, by exploiting the explicit sparseness of the Hamiltonian and density matrices, the computational cost for the construction and storage of the Hamiltonian and the electronic density can be made to scale linearly with the number of atoms, in the limit of large systems. Therefore, a considerable effort has been devoted to obtain orbital bases that would meet the standards of precision of conventional first-principles calculations, while keeping their range as small as possible. A simple scheme for the generation of transferable bases that satisfy both requirements was presented in Refs. 21 and 26. These bases, which we utilize in this work, have been successfully applied to study the ground state properties of very different systems, ranging from insulators to metals, and from bulk to surfaces and nanostructures.[22] It is not obvious, however, that these confined basis sets will be also adequate for the TDDFT calculation of the optical response. In this paper we show that, at least for the two systems considered, the optical absorption can be calculated quite accurately using a basis of NAOs with reasonable confinement radii and a moderate number of orbitals per atom. Our results are in reasonable agreement with other TDDFT calculations using computationally more demanding basis sets or real-space grids.

Our approach is to carry out the calculations in the time domain, explicitly evolving the wave functions. We consider a bounded system in a finite electric field, i.e., the Hamiltonian includes a perturbation $\Delta H = -\mathbf{E}\cdot\mathbf{x}$. For the linear response calculations in this paper we have set the value of this field to 0.01 eV/Å. The system is solved for the ground state using standard time-independent density functional theory.[27] Then we switch off the electric field at time $t=0$, and for every subsequent time step we propagate the occupied Kohn-Sham eigenstates by solving the time-dependent Kohn-Sham equation ($\hbar=1$)

$$i\frac{\partial\Psi}{\partial t} = H\Psi, \tag{4}$$

where H is the time-dependent Hamiltonian given by

$$H = -\frac{1}{2}\nabla^2 + V_{\mathrm{ext}}(\mathbf{r},t) + \int \frac{\rho(\mathbf{r}',t)}{|\mathbf{r}-\mathbf{r}'|}d\mathbf{r}' + V_{\mathrm{xc}}[\rho](\mathbf{r},t). \tag{5}$$

The calculation of the exchange-correlation potential is done using the adiabatic local density approximation (ALDA) where V_{xc} takes the form

$$V_{\mathrm{xc}}[\rho](\mathbf{r},t) \cong \frac{\delta E_{\mathrm{xc}}^{\mathrm{LDA}}[\rho_t]}{\delta\rho_t(\mathbf{r})} = V_{\mathrm{xc}}^{\mathrm{LDA}}[\rho_t](\mathbf{r}). \tag{6}$$

$E_{\mathrm{xc}}^{LDA}[\rho_t]$ is the exchange-correlation energy of the homogeneous electron gas.[28] It is important to notice that the V_{xc} in ALDA is local both in time and space. For every time step we solve Eq. (4), and from the new wavefunctions we construct the new density matrix

$$\rho^{\mu\nu}(t) = \sum_{i}^{\mathrm{occ}} c_i^{\mu}(t)c_i^{\nu}(t), \tag{7}$$

where $c_i^{\mu}(t)$ are the coefficients of the occupied wave functions that correspond to the basis orbitals $\phi_{\mu}(\mathbf{r})$. $\rho^{\mu\nu}(t)$ has to be calculated and stored for overlapping orbitals only. The electron density is then obtained by

$$\rho(\mathbf{r},t) = \sum_{\mu,\nu} \rho^{\mu\nu}(t)\phi_{\mu}(\mathbf{r})\phi_{\nu}(\mathbf{r}) \tag{8}$$

and used for the calculation of the Hamiltonian in the new cycle.

B. Calculation of the polarizabilities

For every time step we calculate the dipole moment $\mathbf{D}(t)$ of the electrons in the cluster. This defines the response to all orders and the frequency-dependent response is found by the Fourier transform

$$\mathbf{D}(\omega) \equiv \int dt\, e^{i\omega t - \delta t} \mathbf{D}(t). \tag{9}$$

In our case we Fourier transform the dipole moment only for $t>0$. It is necessary to include a damping factor δ in order to perform the Fourier transform. This damping factor gives the minimum width of the peaks of the imaginary part of the response. Physically, it can be regarded as an approximate way to account for broadening. To linear order the polarizability is given by $\mathbf{D}(\omega)=\alpha(\omega)\mathbf{E}(\omega)$, so that

$$\mathrm{Im}\,\alpha(\omega) = \omega \frac{\mathrm{Re}\,D(\omega)}{E}, \tag{10}$$

where the field is given by $E(t)=E\,\theta(-t)$. After Fourier transforming the dipole moment we obtain the elements of the frequency-dependent polarizability tensor $\alpha_{ij}(\omega)$. We repeat the calculation with the electric field along different axes unless the symmetry is high enough that this is not needed. The average linear polarizability is given by

$$\langle \alpha(\omega) \rangle = \frac{1}{3} \mathrm{Tr}\,\{\alpha_{ij}(\omega)\}. \tag{11}$$

The choice of the coordinate system does not affect the average polarizability because of the rotational invariance of the trace.

C. Solution of the time-dependent Kohn-Sham equation

Efficient solution of the time-dependent Kohn-Sham equation [Eq. (4)] is of particular interest because together with the calculation of the Hamiltonian, they are the most time-consuming parts of the calculation. In this section we describe our approach of solving Eq. (4).

In the LCAO formalism Eq. (4) takes the form

$$i\frac{\partial c}{\partial t} = S^{-1}Hc, \tag{12}$$

where S is the overlap matrix between the orbitals and c is the column of the coefficients of the local orbitals. The overlap matrix is fixed for a given atomic configuration; hence we have to calculate and invert it only once.

The formal solution of Eq. (12) is

$$c(t) = U(t,0)c(0) = T\exp\left(-i\int_0^t S^{-1}H(t')dt'\right)c(0), \tag{13}$$

where T is the time ordering operator. The most elementary solution is obtained by breaking the total evolution operator into evolution operators of small time durations

$$U(t,0) \simeq \prod_{n=0}^{N-1} U((n+1)\Delta t, n\Delta t), \tag{14}$$

where $\Delta t = T_{\mathrm{tot}}/N$ and

$$U(t+\Delta t, t) = \exp[-iS^{-1}H(t)\Delta t]. \tag{15}$$

T_{tot} is the total time for which we allow the system to evolve. The differences among propagation schemes arise from the way the exponential in Eq. (15) is approximated. In our approach, we approximate the exponential in Eq. (15) with the Crank-Nicholson operator.[29] The coefficients between the steps $n+1$ and n are related by the equation

$$c^{n+1} = \frac{1 - iS^{-1}H(t_n)\Delta t/2}{1 + iS^{-1}H(t_n)\Delta t/2} c^n. \tag{16}$$

This method is unitary, strictly preserving the orthonormality of the states for an arbitrary time evolution. For time-independent Hamiltonians it is also explicitly time reversal invariant and exactly conserves energy. In practice, with a suitable choice of Δt, the energy is satisfactorily conserved even when the Hamiltonian changes with time. For example, in the calculations described below, the drift of the total energy at the end of the simulation ($\sim$20.7 fs in both cases) was only $\Delta E_{\mathrm{tot}}/E_{\mathrm{tot}} \sim 3\times10^{-7}$ for C_{60} and $\sim 8\times10^{-6}$ for Na_8 after $N_{C_{60}} \sim 6100$ and $N_{Na_8} \sim 2800$ time steps, respectively. The larger energy drift in the case of Na_8 is attributed to the use of larger time step. The method is stable when $\Delta t \Delta E_{\max} \ll 1$, where $\Delta E_{\max}$ is the range of the eigenstates of $S^{-1}H$. We can increase the stability of the solution if we include more terms of the expansion in the numerator and denominator of the Crank-Nicholson operator, i.e.,

$$c^{n+1} = \frac{1 - iS^{-1}H\Delta t/2 - 1/2(S^{-1}H\Delta t/2)^2 + i\frac{1}{6}(S^{-1}H\Delta t/2)^3}{1 + iS^{-1}H\Delta t/2 - \frac{1}{2}(S^{-1}H\Delta t/2)^2 - i\frac{1}{6}(S^{-1}H\Delta t/2)^3} c^n. \tag{17}$$

By including more terms in the expansion it is possible either to increase the time step preserving the accuracy or to increase the accuracy of the dynamics and the energy conservation for a given time step. The main advantage of using a bigger time step is the saving of time because we have to calculate the Hamiltonian fewer times. The energy resolution will not be affected since it depends on the total time for which we allow the system to evolve.

There are many advantages associated with the real-time formulation of TDDFT used in this work. Only occupied states are used in the calculation, in contrast to the perturbative approach[18,30] where there is a sum over the excited states

of the system. The implementation is relatively simple, since we use essentially the same operations as already used to find the ground state properties. It is also advantageous that nonlinear effects can be included in a straightforward way as shown in Sec. IV. The merit of the real-time approach becomes more transparent in the case of the calculation of the nonlinear polarizabilities because the perturbative approach involves multiple sums over the excited states, something which is computationally very demanding. One disadvantage of the real-time approach is the calculation of the Hamiltonian for every time step. Although this is not an attractive feature there is no other way to calculate the time evolution of the system.

The method presented in this work has many similarities with that described by Yabana and Bertsch,[15] the main difference being our use of a LCAO basis set in the present case compared to their method in the which the states are represented on a regular grid in real space. Yabana and Bertsch use the same real-space method as Vasiliev and co-workers[17] in which the action of the Hamiltonian on a state is done by approximating the Laplacian operator using a finite difference expression. Even though the operators are sparse and easy to apply, the representation of the states requires much greater computer memory, especially for large systems and for systems with atoms that require finely spaced grids.

III. DISCUSSION OF RESULTS

A. Small metal clusters: Na_8

The first calculation we performed is the optical response of Na_8. The main purpose of this calculation was to investigate the accuracy of our method in the case of a small cluster, where the effects related to the confinement of the orbitals should be more noticeable and where the size of our basis is much smaller than that in previous calculations using real-space grids.[17] It has to be kept in mind that the calculation of the optical response of Na_8 is just a test case since the method of calculation used is intended for large clusters where we benefit from the order-N features of SIESTA. The calculation of the optical response of Na_8 is a difficult test for codes that use localized orbitals, such as SIESTA, because it has very delocalized wave functions and consequently a very delocalized density distribution. Na_8 is the smallest closed shell Na cluster with an optical response that exhibits the presence of a plasmon experimentally observed at 2.53 eV.[31,32] The width of the plasmon is due to Landau damping.[33]

Previous work can be grouped into two types: earlier work on jellium spheres[31,33–35] that reproduces the qualitative features but not the quantitative energies of the peaks, and more recent work[14,17,36] that takes into account the detailed atomic structure and is in general in very good agreement with experiment.[31,32] In the first category are the calculations of Selby and co-workers,[31,34] who calculated the photoabsorption cross section using the modified Mie theory, which is a classical theory. The plasmon was found to be at ~ 2.76 eV. By using the self-consistent jellium model in the TDLDA, first introduced by Ekardt,[33] Yannouleas *et al.*[35] calculated the photoabsorption cross section of Na_8 and predicted the plasmon position at 2.82 eV.

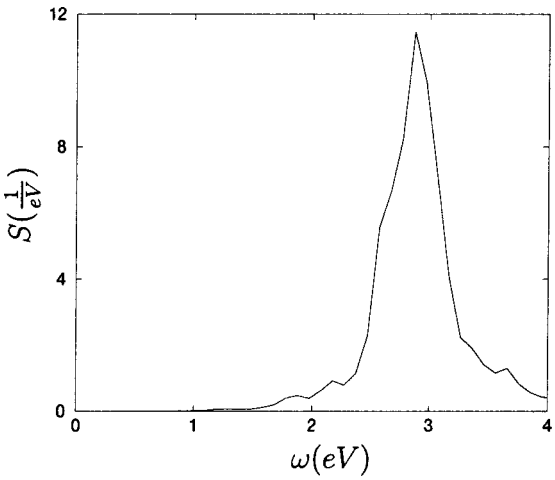

FIG. 1. Dipole strength function of Na_8 vs energy.

Bounačić-Koutecký *et al.*[36] calculated the absorption spectrum of Na_8 using the configuration-interaction method (CI). Because the all-electron calculation is computationally very demanding, they obtained the excited states by a nonempirical effective core potential corrected for the core-valence correlation using a core polarization potential. The position of the plasmon was predicted at ~ 2.55 eV. Rubio *et al.*[14] calculated the photoabsorption cross section within TDLDA. Their results are in excellent agreement with experiment. In particular, the position of the plasmon was found at 2.55 eV. Vasiliev *et al.*[17] calculated the photoabsorption cross section using TD-DFRT.[18] Their calculations made use of norm-conserving pseudopotentials and a real-space grid of points. The position of the plasmon agreed with the photoabsorption experiments of Selby *et al.*[31] and Wang *et al.*[32] within 0.1–0.2 eV.

In our calculation we let the system evolve for the total time of $T=31.42\ \text{eV}^{-1}$. The energy resolution, determined by $\Delta\omega=\pi/T$, is, in consequence, equal to 0.1 eV. The time step is $11.025\times10^{-3}\ \text{eV}^{-1}$, and the damping factor used in the Fourier transform is 0.095 eV. Troullier-Martins pseudopotentials[23] including nonlinear partial core corrections[37] for the exchange-correlation interaction between valence and core electrons and an auxiliary real-space grid[20] equivalent to a plane-wave cutoff of 70 Ry are also used in this calculation. The basis set includes 13 NAOs per atom: two radial shapes to represent the $3s$ states plus a polarization[21] p shell with confinement radii $r_s=r_p^{\text{pol}}=12.2$ a.u. and two additional $3p$ and $3d$ shells with radii $r_p=r_d=10.0$ a.u.

Figures 1 and 2 present, respectively, our results for the dipole strength function and the imaginary part of the linear polarizability of Na_8 for energies up to 4 eV. The shape of these curves is in good agreement with both the calculations of Vasiliev *et al.*[17] and the experiments of Wang *et al.*[32] However, the results appear to be shifted to higher energies. In fact, the maximum of the plasmon peak is obtained at 2.8 eV, which is 0.27 eV higher than the experimentally observed value. This shift to higher energies seems to be related

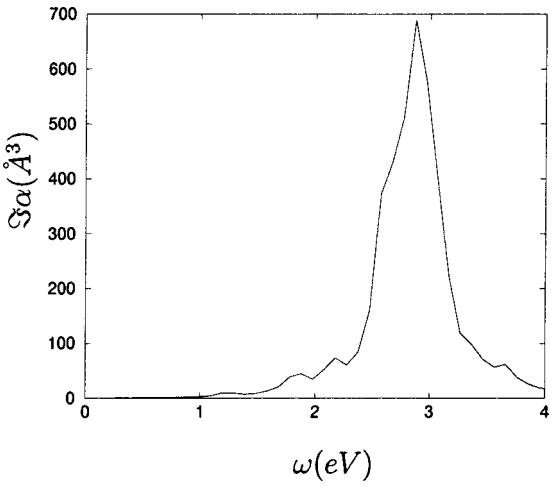

FIG. 2. Imaginary part of the linear polarizability of Na_8 vs energy.

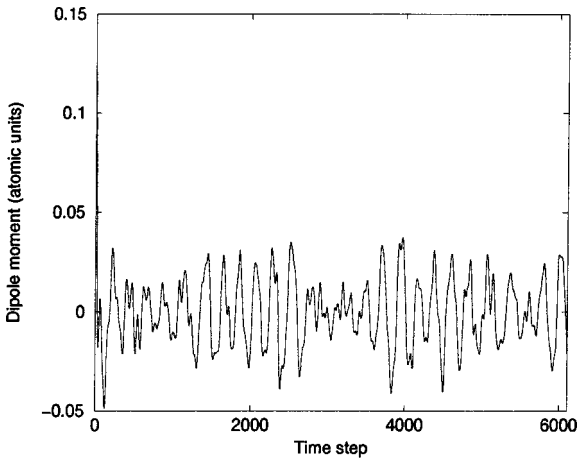

FIG. 3. Dipole moment of C_{60} vs number of time steps.

to the extension of the LCAO basis: using more confined orbitals we get a larger shift. The integrated dipole strength is equal to 6.97 out of 8, thus fulfilling 87.13% of the sum rule. The partial fulfillment of the sum rule signifies the incompleteness of our basis set. The static linear polarizability $\alpha(0)$ can be obtained from standard (static) calculations of the induced dipole as a function of the applied field. Using this approach we obtain a value of 13.2 Å^3/atom. An alternative way to calculate $\alpha(0)$ is provided by the formula

$$\alpha(0)=\frac{e^2\hbar}{m}\int_0^\infty \frac{S(\omega)d\omega}{\omega^2}=\frac{2}{\pi}\int_0^\infty \frac{\mathrm{Im}\,\alpha(\omega)}{\omega}d\omega, \quad (18)$$

from which we obtain a value of 12.5 Å^3/atom. [This result can also be derived from the fact that for the step perturbation $D(t=0)=\alpha(0)E$.] The discrepancy between both estimations is probably related to the lack of energy resolution of the calculated $\alpha(\omega)$ to perform the integral in Eq. (18) with the required accuracy. Both results are in reasonable agreement with the experimental value of 15.4 Å^3/atom reported by de Heer,[38] of 14.9 Å^3/atom computed by Rubio *et al.*[14] using TDLDA, and of 14.6 Å^3/atom and 14.7 Å^3/atom calculated by Vasiliev *et al.*[17,39] using the TDLDA and finite field methods, respectively.

B. Large molecules: C_{60}

The best known fullerene C_{60} is a very interesting system with strong electron-electron interactions due to the confinement. There are quite a few calculations concerning the optical properties of C_{60} and in particular its optical response but only few of them are *ab initio*. The main feature of the optical response of C_{60} is the presence of two collective excitations (plasmons). The low-energy plasmon can be associated with the π electrons while the high-energy plasmon with both the σ and π electrons, in analogy with the plasmons in graphite.[40,41] The plasmons have been observed in a plethora of experiments.[42–46]

The earliest theoretical work[47–50] on C_{60} involved simplifying approximations for the electron states (tight-binding or spherical averaging) and for the electron interaction [neglect of screening effects or random phase approximation (RPA) treatments]. We will compare our results with those of Westin *et al.*[51] and Yabana and Bertsch,[15] who used large basis sets and realistic carbon potentials. Westin *et al.* used single-particle wave functions, determined from a local density approximation (LDA) calculation, to evaluate the dipole matrix elements which combined with a sum over states approach yielded the unscreened frequency-dependent linear polarizability. Screening was included in a RPA-like fashion by introducing an effective screening parameter. The polarizability calculated in the static limit was used to evaluate this parameter for the calculation of the dynamic response. The optical response and the sum rule for the low-energy part were in reasonable agreement with the experiment of Leach *et al.*[46] Yabana and Bertsch[15] used TDLDA, evolving the system in real space and time, to calculate the dipole strength function of C_{60}. Their calculation also gives reasonable agreement with the experimental data of Leach *et al.*[46] for the sum rule of the low-energy part although it misses many details of the structure.

The total simulation time in our calculation of the polarizability and dipole strength of the C_{60} molecule is again 31.416 eV^{-1}, and the corresponding energy resolution is 0.1 eV. The time step, however, which is set equal to 5.145×10^{-3} eV^{-1}, is smaller than the one used for Na_8. This is because of the higher frequency range of the response of C_{60}. The damping factor used in the Fourier transform is equal to 0.34 eV in this case. Troullier-Martins pseudopotentials,[23] a double-ζ polarized basis set, and a real-space grid cutoff[20] of 70 Ry were used in this calculation. There are 13 NAOs per C atom: two different radial shapes for the description of the $2s$ states, another two for the $2p$, plus an additional shell of d orbitals. The radii of confinement used are $r_s=5.12$ a.u. and $r_p=r_d^{pol}=6.25$ a.u. (corresponding to an *energy shift*[21] of 50 meV). For C_{60}, the calculated spectra show a small dependence in these radii, at least as far as they are not selected to be very stringent.

In Fig. 3, the dipole moment is shown as a function of the time step number. The dipole strength function obtained from the time evolution of the dipole moment is shown in

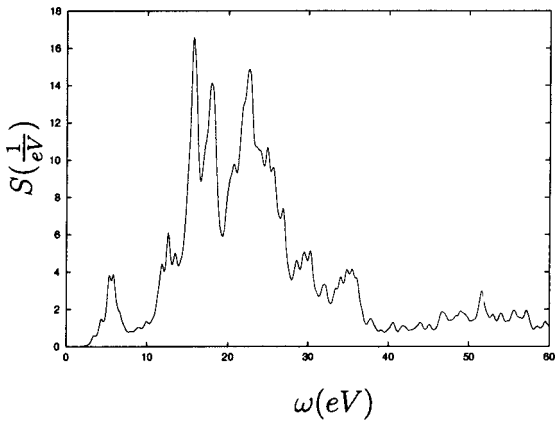

FIG. 4. Dipole strength function of C_{60} vs energy.

Fig. 4 for energies up to 60 eV. Its main features are the low-energy transitions that come from the π electrons and the σ and π electron transitions in the region of 14–27 eV. In the low-energy part of dipole strength function we have peaks at 3.5, 4.4, 5.4, and 5.8 eV, which agree very well with the ones obtained by the experiments of Bauernschmitt *et al.*[52] and by the calculations of Westin *et al.*[51] By integrating the dipole strength function over energy we get the sum rule strength. The total sum rule strength is 223.78 out of 240. Therefore, we satisfy the sum rule up to 93.24%. This reflects the incompleteness of our basis set, which fails to reproduce some of the excitations in the high-energy part of the spectrum. The σ plasmon is broadened, but this is a common feature of all the TDDFT calculations done for C_{60}.[15]

In Fig. 5, the imaginary part of the polarizability is given as function of energy. By using Eq. (18), the static linear polarizability $\alpha(0)$ is found to be 91.1 Å^3, while our finite field calculations produce a value of 87.3 Å^3. Results for $\alpha(0)$, from accurate finite-field calculations using fifteen values of the field, are given in Sec. IV. Both values are higher than the lower limit estimation of 62.5 Å^3 from quantum-mechanical calculations,[53] and in reasonable agreement with the value of 85 Å^3 obtained by Yabana and Bertsch.[15] They also agree with the experimental values of

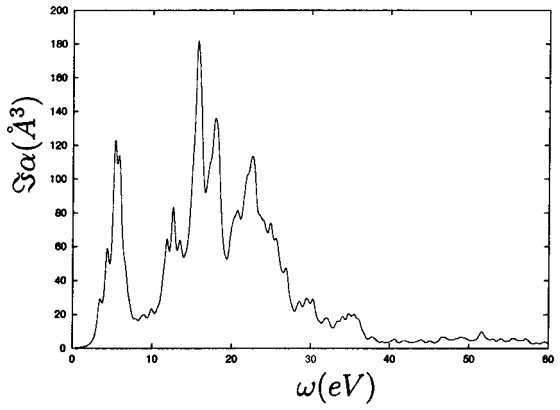

FIG. 5. Imaginary part of the linear polarizability of C_{60} vs energy.

88.2 Å^3 given by Meth *et al.*,[54] 79.3 Å^3 from uv absorption,[55] and 85.2 Å^3 from electron energy loss spectra.[56,57]

IV. NONLINEAR POLARIZABILITIES

Because of the nonperturbative nature of our method we are able, for large values of the applied field, to obtain nonlinear polarizabilities. In this section, we develop a method for the calculation of the imaginary part of the integrated frequency-dependent second-order nonlinear polarizability, $\mathrm{Im}\,\tilde{\gamma}_{\mathrm{step}}(\omega)$, which is related to the response to a step function, and apply it to C_{60}. Because C_{60} is centrosymmetric the first-order nonlinear polarizability, $\beta(\omega)$, and all other polarizabilities involving an even number of fields vanish by symmetry.

The advantage of the explicit time method to study the nonlinear response is that we use exactly the same operations as in the linear case. It is also much simpler than the perturbative approach, which involves multiple sums over the excited states, something extremely computationally demanding, especially for large systems. The disadvantage is that (unlike the linear case where each Fourier component is independent) the nonlinear response depends upon the detailed spectrum of the applied field. Here we derive the nonlinear response of an electric field coupled to C_{60} for the case where the field is the step function used before. A different calculation would have to be done to find the nonlinear response to a field with a different time dependence.

First we give the relation of our calculation to the general definition of second-order nonlinear response, as a function of time, which is[58]

$$D^{(3)}(t)=\int_{-\infty}^{t}dt_1\int_{-\infty}^{t_1}dt_2\int_{-\infty}^{t_2}dt_3\,\gamma(t;t_1,t_2,t_3)\times E(t_1)E(t_2)E(t_3). \tag{19}$$

For the case of a step function perturbation, i.e., $E(t)=E\theta(-t)$, it takes the form

$$D^{(3)}(t)=iE^3\lim_{\delta_i\to 0^+}\int\frac{d\omega_1 d\omega_2 d\omega_3}{(2\pi)^3}\times\frac{e^{-i(\omega_1+\omega_2+\omega_3)t}\gamma(-\omega_1-\omega_2-\omega_3;\omega_1,\omega_2,\omega_3)}{(\omega_1-i\delta_1)(\omega_2-i\delta_2)(\omega_3-i\delta_3)}. \tag{20}$$

We Fourier transform Eq. (20) and obtain the second-order nonlinear response as a function of frequency

$$D^{(3)}(\omega)=iE^3\lim_{\delta_i\to 0^+}\int\frac{d\omega_2 d\omega_3}{(2\pi)^2}\times\frac{\gamma(-\omega;\omega-\omega_2-\omega_3,\omega_2,\omega_3)}{(\omega-\omega_2-\omega_3-i\delta_1)(\omega_2-i\delta_2)(\omega_3-i\delta_3)}. \tag{21}$$

The quantity we calculate is the real part of the second-order nonlinear response, $\mathrm{Re}\,D^{(3)}(\omega)$, from which we can extract the imaginary part of the integrated second-order nonlinear polarizability, $\mathrm{Im}\,\tilde{\gamma}_{\mathrm{step}}(\omega)$. Explicit details are given below and in analogy to Eq. (10) $\mathrm{Im}\,\tilde{\gamma}_{\mathrm{step}}(\omega)$ is given by

$$\mathrm{Im}\,\tilde{\gamma}_{\mathrm{step}}(\omega) = -\omega \lim_{\delta_i \to 0^+} \mathrm{Im} \int \frac{d\omega_2 d\omega_3}{(2\pi)^2} \times \frac{\gamma(-\omega;\omega-\omega_2-\omega_3,\omega_2,\omega_3)}{(\omega-\omega_2-\omega_3-i\delta_1)(\omega_2-i\delta_2)(\omega_3-i\delta_3)} = \omega \frac{\mathrm{Re}\,D^{(3)}(\omega)}{E^3}. \quad (22)$$

Just as in Eq. (18) for the linear term, $\mathrm{Im}\,\tilde{\gamma}_{\mathrm{step}}(\omega)$ can be related to the static second-order nonlinear polarizability by the expression

$$\frac{2}{\pi}\int_0^\infty \frac{d\omega}{\omega}\mathrm{Im}\,\tilde{\gamma}_{\mathrm{step}}(\omega) = \gamma(0;0,0,0). \quad (23)$$

Equation (23) can be trivially derived by realizing that $D^{(3)}(t=0)=\gamma(0;0,0,0)E^3$ when a step function perturbation is applied. Alternatively, we can derive Eq. (23) directly from Eq. (21) by applying the Kramers-Kroning relations for $\gamma(-\omega_1-\omega_2-\omega_3;\omega_1,\omega_2,\omega_3)$. In fact, with the help of the Kramers-Kroning relations we can derive another interesting equality for the integrated response,

$$\frac{1}{3}\int d\omega\,\mathrm{Im}\,\tilde{\gamma}_{\mathrm{step}}(\omega) = \int d\omega\,\mathrm{Im}\,\gamma(-\omega;\omega,0,0). \quad (24)$$

In order to determine $\tilde{\gamma}_{\mathrm{step}}(\omega)$ we calculate the response of the system with step function perturbations having two different magnitudes. In this case we use a more complete basis set than for the linear polarizability because the calculation of nonlinear effects is more demanding. In addition to the 13 NAOs per C atom given previously, we have added two orbitals per atom with different radial shapes (double-ζ) having $3s$ character (since we are using pseudopotentials this really means orbitals with one radial node). The radial confinement is chosen to be $r_{3s}=6.57$ a.u. Other reasonable choices of r_{3s} do not change the results substantially. The inclusion of the $3s$ states does not lead to important changes the the absorption spectrum and the value of the static linear polarizability, but it does change the static nonlinear polarizability which is sensitive to the way the high-frequency part of the spectrum changes with the field strength, as shown in Eq. (23). In the first calculation, the field used is equal to $E_1=0.10$ V/Å, and we assume that the response $D_1(\omega)$ is linear with respect to the field. This assumption was verified at $\omega=0$ where the nonlinear contribution to the response only 5.13×10^{-3}%. The contribution is of the same order of magnitude for $\omega\neq0$. In the second calculation the field is equal to $E_2=1.00$ V/Å, and we assume that the response $D_2(\omega)$ consists of the linear response and the second-order

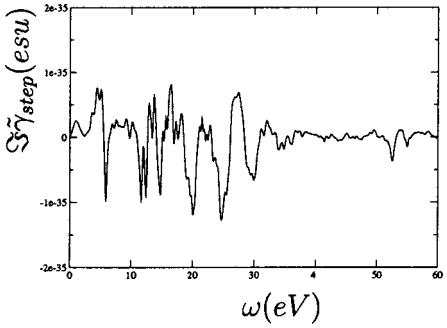

FIG. 6. Imaginary part of the integrated second order nonlinear polarizability, $\mathrm{Im}\,\tilde{\gamma}_{\mathrm{step}}(\omega)$, of C_{60} vs energy.

nonlinear response $D_2^{(3)}(\omega)$. The values of the field are in the same range as those used by Westin *et al.*[51] for the determination of the static second-order nonlinear polarizability. Using Eq. (10), we have

$$D_1(\omega)=\alpha(\omega)E_1(\omega)=\alpha(\omega)\frac{E_1}{i\omega} \quad (25)$$

and

$$D_2(\omega)-\alpha(\omega)E_2(\omega)=D_2^{(3)}(\omega). \quad (26)$$

From Eq. (22) it follows that

$$D_2^{(3)}(\omega)=\frac{\tilde{\gamma}_{\mathrm{step}}(\omega)}{i\omega}E_2^3, \quad (27)$$

and from Eqs. (25), (26), and (27) we obtain

$$\tilde{\gamma}_{\mathrm{step}}(\omega)=\frac{i\omega}{E_2^3}\left(D_2(\omega)-\frac{E_2}{E_1}D_1(\omega)\right). \quad (28)$$

Our calculation for $\tilde{\gamma}_{\mathrm{step}}(\omega)$ is quite straightforward in contrast to the perturbative method where it becomes computationally very demanding.

In Fig. 6, we present the results, up to 60 eV, for $\mathrm{Im}\,\tilde{\gamma}_{\mathrm{step}}(\omega)$, where $\mathrm{Im}\,\tilde{\gamma}_{\mathrm{step}}(\omega)$ is given by Eq. (22). As expected, $\mathrm{Im}\,\tilde{\gamma}_{\mathrm{step}}(\omega)$ has both positive and negative values. The reason why $\mathrm{Im}\,\tilde{\gamma}_{\mathrm{step}}(\omega)$ does not vanish below some finite frequency (as does the linear response) is because the second-order nonlinear term represents many processes of both absorption and emission of photons and the C_{60} molecule can couple to a continuum of modes that extends to zero frequency. This can also be seen in the integral expression, Eq. (22). The value of the static $\gamma(0;0,0,0)$ satisfies Eq. (23) and is found to be 6.3×10^{-36} esu in our calculation.

The static nonlinear polarizability $\gamma\equiv\gamma(0;0,0,0)$ can also be calculated directly from the usual static self-consistent calculations performed for a range of finite fields. This value can be compared to similar calculations in the literature and it provides an internal consistency test for our calculation of the integrated frequency-dependent second-order nonlinear polarizability. We have followed here a procedure similar to that used in Ref. 59, performing LDA calculations of the total energy and electric dipole of the C_{60} molecule for fif-

teen different values of an external static electric field E ranging from 0.005 V/Å to 2.0 V/Å. The results of the total energy were then fitted using the expression $W_{\rm tot} = W_0 - \frac{1}{2}\alpha E^2 - \frac{1}{4}\gamma E^4$, where α is the linear polarizability and γ the second-order nonlinear polarizability. The values obtained for α and γ are, respectively, 89.5 Å^3 and 6.5 $\times 10^{-36}$ esu. The results for the dipole moment were fitted to the expression $D = \alpha E + \gamma E^3$, leading to 89.6 Å^3 and 5.9 $\times 10^{-36}$ esu. These values of γ are in reasonable agreement with the value of 6.3×10^{-36} esu obtained using Eq. (23) and provide an estimate of the consistency and accuracy of our calculations.

Our results for γ are in generally good agreement with previous static LDA calculations, although our results are somewhat smaller. Quong and Pederson[59] reported values of 82.7 Å^3 and 7.0×10^{-36} esu, for α and γ, respectively, using an all-electron method with a Gaussian expansion as a basis set. van Gisbergen *et al.*[16] reported very similar values, 82.5 Å^3 and 7.3×10^{-36} esu, using a computational scheme based on a frozen-core approximation and a basis set of Slater functions. In the latter work special care was taken to add delocalized orbitals. Larger values are found in calculations that use more complete basis sets [9.6×10^{-36} esu (Ref. 61)] and real-space grids [10.4×10^{-36} esu) (Ref. 62)]. Results obtained using simplified tight-binding models within an independent electron picture, where the effects of screening are neglected, lead to much larger values of γ of the order of 200×10^{-36} esu.[63–65] The experimental value is not known, but an experimental upper bound of 3.7×10^{-35} esu has been proposed by Geng and Wright,[60] which is larger than all the theoretical estimates.

We conclude that the small value of γ from our calculation can be attributed to (i) the incompleteness of our basis set and (ii) the fact that the major contribution to the optical absorption spectrum of C_{60} comes from the higher excited states.[56] The role of the extended orbitals is to complete the basis set and provide a better description of the high-energy spectra (above the ionization energy), which also has an important effect upon the real part of the second-order nonlinear polarizability γ. Incomplete treatment of delocalized states is a limitation of the basis set used in this work. We emphasize, however, that the major conclusions of our work are the spectra given for C_{60} in Figs. 5 and 6. The important low-energy features are essentially unchanged by the extended orbitals so that the small basis used here is sufficient.

V. CONCLUSION

We presented a method for the calculation of the optical response of atoms and clusters. The main features of the method are the description of the wave functions in terms of an efficient local orbital (LCAO) basis and the explicit evolution of the system in time. This approach is designed for large clusters and in fact it gives good results for C_{60}. It is also shown to work reasonably well even for small systems, such as Na_8. Our approach has the desirable features that only occupied states are needed and that the most computationally intensive operations are essentially the same as those used to calculate the ground state properties. In addition, nonlinear effects can be included in a straightforward way. We developed a method for the calculation of the nonlinear response, which is considerably simpler than the perturbative approach which involves multiple sums over the excited states. We also presented results from the calculation of the second-order nonlinear response of C_{60}.

ACKNOWLEDGMENTS

We would like to thank Professor L. Cooper for useful discussions, and Dr. I. Vasiliev for reading the manuscript. This material is based upon work supported by the U.S. Department of Energy, Division of Material Sciences under Award No. DEFG02-91ER45439, through the Frederick Seitz Materials Research Laboratory at the University of Illinois at Urbana-Champaign.

*Present address: Departamento de Física de Materiales and DIPC, Facultad de Química, UPV/EHU, Apdo. 1072, E-20080 San Sebastián, Spain.

[1] P. Hohenberg and W. Kohn, Phys. Rev. **136**, B864 (1964).
[2] W. Kohn and L. J. Sham, Phys. Rev. **140**, A1133 (1965).
[3] A. Zangwill and P. Soven, Phys. Rev. A **21**, 1561 (1980).
[4] B. M. Deb and S. K. Ghosh, J. Chem. Phys. **77**, 342 (1982).
[5] S. K. Ghosh and B. M. Deb, Chem. Phys. **71**, 295 (1982).
[6] L. J. Bartolotti, Phys. Rev. A **24**, 1661 (1981).
[7] L. J. Bartolotti, Phys. Rev. A **26**, 2243 (1982).
[8] E. Runge and E. K. U. Gross, Phys. Rev. Lett. **52**, 997 (1984).
[9] E. K. U. Gross and W. Kohn, Phys. Rev. Lett. **55**, 2850 (1985).
[10] D. Mearns and W. Kohn, Phys. Rev. A **35**, 4796 (1987).
[11] E. K. U. Gross, C. A. Ullrich, and U. J. Gossmann, in *Density Functional Theory*, edited by E. K. U. Gross and R. M. Dreizler (Plenum Press, New York, 1995).
[12] E. K. U. Gross, J. F. Dobson, and M. Petersilka, in *Topics in Current Chemistry*, edited by R. F. Nalewajski (Springer-Verlag, Berlin Heidelberg, 1996), Vol. 181.
[13] A. Rubio, J. A. Alonso, X. Blase, and S. G. Louie, Int. J. Mod. Phys. B **11**, 2727 (1997).
[14] Angel Rubio, J. A. Alonso, X. Blase, L. C. Balbás, and Steven G. Louie, Phys. Rev. Lett. **77**, 247 (1996).
[15] K. Yabana and G. F. Bertsch, Phys. Rev. B **54**, 4484 (1996).
[16] S. J. A. van Gisbergen, J. G. Snijders, and E. J. Baerends, Phys. Rev. Lett. **78**, 3097 (1997).
[17] I. Vasiliev, S. Öğüt, and J. R. Chelikowsky, Phys. Rev. Lett. **82**, 1919 (1999).
[18] M. E. Casida, in *Recent Developments and Applications of Modern Density Functional Theory*, edited by J. M. Seminario (Elsevier, Amsterdam, 1996).
[19] M. Moseler, H. Häkkinen, and Uzi Landman, Phys. Rev. Lett. **87**, 053401 (2001).
[20] D. Sánchez-Portal, P. Ordejón, E. Artacho, and J. M. Soler, Int. J. Quantum Chem. **65**, 453 (1997).
[21] E. Artacho, D. Sánchez-Portal, P. Ordejón, A. García, and J. M. Soler, Phys. Status Solidi B **215**, 809 (1999).
[22] P. Ordejón, Phys. Status Solidi B **217**, 335 (2000).

[23] N. Troullier and J. L. Martins, Phys. Rev. B **43**, 1993 (1991).
[24] L. Kleinman and D. M. Bylander, Phys. Rev. Lett. **48**, 1425 (1982).
[25] O. F. Sankey and D. J. Niklewski, Phys. Rev. B **40**, 3979 (1989); D. Sánchez-Portal, E. Artacho, and J. M. Soler, J. Phys.: Condens. Matter **8**, 3859 (1996).
[26] J. Junquera, O. Paz, D. Sánchez-Portal, and E. Artacho, Phys. Rev. B **64**, 235111 (2001).
[27] Our calculations are performed using a supercell geometry. Therefore, we are talking here about the ground state of a bounded system in the presence of a periodic triangular potential, with slope E. This provides a meaningful model for a cluster in the presence of a finite electric field only if $|E|<|E_c|$, where the critical slope depends on the system under consideration, and on the lateral size of the simulation cell L. In particular, $E_c \rightarrow 0$ when $L\rightarrow\infty$. In our case this problem is mitigated by the use of basis orbitals localized in regions relatively close to the atoms; we can therefore use quite high electric fields in our calculations and still get meaningful solutions.
[28] D. M. Ceperley and B. J. Alder, Phys. Rev. Lett. **45**, 566 (1980).
[29] R. S. Varga, *Matrix Iterative Analysis* (Prentice-Hall, Englewood Cliffs, NJ, 1962), p. 263.
[30] H. Ehrenreich and M. H. Cohen, Phys. Rev. **115**, 786 (1959).
[31] K. Selby, M. Vollmer, J. Masui, V. Kresin, W. A. de Heer, and W. D. Knight, Phys. Rev. B **40**, 6417 (1989).
[32] C. R. C. Wang, S. Pollack, D. Cameron, and M. M. Kappes, J. Chem. Phys. **93**, 3787 (1990).
[33] W. Ekardt, Phys. Rev. Lett. **52**, 1925 (1984).
[34] W. A. de Heer, K. Selby, V. Kresin, J. Masui, M. Vollmer, A. Châtelain, and W. D. Knight, Phys. Rev. Lett. **59**, 1805 (1987).
[35] C. Yannouleas, R. A. Broglia, M. Brack, and P. F. Bortignon, Phys. Rev. Lett. **63**, 255 (1989).
[36] V. Bonačić-Koutecký, P. Fantucci, and J. Koutecký, J. Chem. Phys. **93**, 3802 (1990).
[37] S. G. Louie, S. Froyen, and M. L. Cohen, Phys. Rev. B **26**, 1738 (1982).
[38] W. A. de Heer, Rev. Mod. Phys. **65**, 611 (1993).
[39] I. Vasiliev, S. Öğüt, and J. R. Chelikowsky, Phys. Rev. Lett. **78**, 4805 (1997).
[40] I. L. Spain, Chem. Phys. Carbon **16**, 119 (1980).
[41] Y. Saito, H. Shinohara, and A. Ohsita, Jpn. J. Appl. Phys., Part 2 **30**, L1068 (1991).
[42] H. Ajie, M. M. Alvarez, S. J. Anz, R. D. Beck, F. Diederich, K. Fostiropoulos, D. R. Huffman, W. Kratschmer, Y. Rubin, K. E. Schriver, D. Sensharma, and R. L. Whetten, J. Phys. Chem. **94**, 8630 (1990).
[43] J. R. Heath, R. F. Curl, and R. E. Smalley, J. Chem. Phys. **87**, 4236 (1987).
[44] J. W. Keller and M. A. Coplan, Chem. Phys. Lett. **193**, 89 (1992).
[45] I. V. Hertel, H. Steger, J. de Vries, B. Weisser, C. Menzel, B. Kamke, and W. Kamke, Phys. Rev. Lett. **68**, 784 (1992).
[46] S. Leach, M. Vervloet, A. Desprès, E. Bréheret, J. Hare, T. J. Dennis, H. W. Kroto, R. Taylor, and D. R. M. Walton, Chem. Phys. **160**, 451 (1992).
[47] G. F. Bertsch, A. Bulgac, D. Tománek, and Y. Wang, Phys. Rev. Lett. **67**, 2690 (1991).
[48] A. Rubio, J. A. Alonso, and J. M. López, Physica B **183**, 247 (1993).
[49] A. Bulgac and N. Ju, Phys. Rev. B **46**, 4297 (1992).
[50] F. Alasia, R. A. Broglia, H. E. Roman, L. I. Serra, G. Colò, and J. M. Pacheco, J. Phys. B **27**, L643 (1994).
[51] E. Westin, A. Rosén, G. Te Velde, and E. J. Baerends, J. Phys. B **29**, 5087 (1996).
[52] R. Bauernschmitt, R. Ahlrichs, F. H. Hennrich, and M. M. Kappes, J. Am. Chem. Soc. **120**, 5052 (1998).
[53] P. W. Fowler, P. Lazzeretti, and R. Zanasi, Chem. Phys. Lett. **165**, 79 (1990).
[54] J. S. Meth, H. Vanherzeele, and Y. Wang, Chem. Phys. Lett. **197**, 26 (1992).
[55] S. L. Ren, Y. Wang, A. M. Rao, E. McRae, J. M. Holden, T. Hager, K. Wang, Wen-Tse Lee, W. F. Ni, J. Selegue, and P. C. Eklund, Appl. Phys. Lett. **59**, 2678 (1991).
[56] E. Sohmen, J. Fink, and W. Krätschmer, Z. Phys. B: Condens. Matter **86**, 87 (1992).
[57] H. Cohen, E. Kolodney, T. Maniv, and M. Foldman, Solid State Commun. **81**, 183 (1992).
[58] C. Flytzanis, in *Quantum Electronics*, edited by H. Rabin and C. L. Tang (Academic Press, New York, 1975).
[59] A. A. Quong and M. R. Pederson, Phys. Rev. B **46**, 12 906 (1991).
[60] Lei Geng and J. C. Wright, Chem. Phys. Lett. **249**, 105 (1996).
[61] P. Norman, Y. Luo, D. Jonsson, and H. Ågren, J. Chem. Phys. **106**, 8788 (1997).
[62] J.-I. Iwata, K. Yabana, and G. F. Bertsch, J. Chem. Phys. **115**, 8773 (2001).
[63] Z. Shuai and J. L. Brédas, Phys. Rev. B **46**, 16 135 (1992).
[64] K. Harigaya and S. Abe, Jpn. J. Appl. Phys., Part 2 **31**, L887 (1992).
[65] J. Dong, J. Jiang, J. Yu, Z. D. Wang, and D. Y. Xing, Phys. Rev. B **52**, 9066 (1995).